THE CATALYTIC DIVERSITY OF RNAS

*Martha J. Fedor**‡ and James R. Williamson**‡§

Abstract | The natural RNA enzymes catalyse phosphate-group transfer and peptide-bond formation. Initially, metal ions were proposed to supply the chemical versatility that nucleotides lack. In the ensuing decades, structural and mechanistic studies have substantially altered this initial viewpoint. Whereas self-splicing ribozymes clearly rely on essential metal-ion cofactors, self-cleaving ribozymes seem to use nucleotide bases for their catalytic chemistry. Despite the overall differences in chemical features, both RNA and protein enzymes use similar catalytic strategies.

RIBOZYME
An enzyme in which RNA functions as the catalytic component.

GROUP-I SELF-SPLICING INTRONS
A group of catalytic RNAs that carry out phosphodiester-cleavage and -ligation reactions, which result in the removal of noncoding intronic sequences and splicing of coding exon sequences. Group-I introns were the first class of catalytic RNAs to be discovered.

S_N2-TYPE IN-LINE MECHANISM
The chemical term for a class of nucleophilic substitution reactions that involve a concerted attack of a nucleophile and the departure of a leaving group.

**Department of Molecular Biology, ‡the Skaggs Institute for Chemical Biology, and the §Department of Chemistry, Scripps Research Institute, 10550 North Torrey Pines Road, La Jolla, California 92037, USA.*
e-mails: mfedor@scripps.edu; jrwill@scripps.edu
doi:10.1038/nrm1647

Catalytic RNAs — or RIBOZYMES — provide a window into a primordial 'RNA world' from which 'modern' biology might have evolved[1]. Contemporary roles for RNA catalysis in the modern protein world can still be found in the regulation of gene expression and in protein synthesis[2–5]. Several recent high-resolution structures of self-cleaving and self-splicing RNAs have provided close-up views of the active sites of the hammerhead[6–12], hepatitis delta virus (HDV)[13,14] and hairpin[15,16] self-cleaving RNAs and GROUP-I SELF-SPLICING INTRONS[17–20]. The structure of the ribosome[3] has given us a picture of the peptidyl-transferase centre, which is the ribosome active site[21,22]. Numerous mechanistic studies that have been carried out over more than 20 years since ribozymes were first discovered can now be compared and contrasted with the corresponding structures, providing new insights into how RNA enzymes use their functional groups for catalysis.

Naturally occurring ribozymes catalyse phosphate-group transfer through two types of chemical reaction that differ in their reaction products (BOX 1). The small self-cleaving RNAs catalyse reversible phosphodiester-cleavage reactions that generate 5′-hydroxyl and 2′–3′-cyclic-phosphate termini. Ribonuclease (RNase) P — the ubiquitous ribozyme that is responsible for cleaving 5′-flanking sequences from precursor tRNAs — and self-splicing introns catalyse phosphodiester-cleavage and -ligation reactions that produce 5′-phosphate and 3′-hydroxyl termini. Both kinds of phosphoryl-transfer reaction proceed with an inversion of the configuration of the stereochemically distinct nonbridging oxygens that are bound to the chiral phosphorus undergoing nucleophilic attack, which indicates an S_N2-TYPE IN-LINE ATTACK MECHANISM (BOX 1).

Efforts to understand enzyme reaction mechanisms are guided by TRANSITION-STATE THEORY and the principle that a catalyst functions by lowering the energy barrier between the transition state and the ground state of the reactants. For ribozymes, possible catalytic strategies include: positioning the reactive groups in an optimal alignment; GENERAL ACID–BASE catalysis of proton transfer to activate nucleophilic oxygens or to stabilize oxyanion leaving groups; electrostatic catalysis through the stabilization of negative charge that accumulates in the transition state; or destabilization of the ground state[23,24].

Over the years, RNA enzymologists have endeavoured to understand which of these catalytic strategies are used by RNA enzymes. In contrast to the chemical versatility of the amino-acid side chains that comprise the active sites of protein enzymes, just four nucleotides are available for the construction of the ribozyme active sites. Amino acids can contribute various nonpolar, charged and uncharged polar side chains for general acid–base and electrostatic catalysis. In protein enzymes that catalyse similar phosphate-group transfer reactions, positively charged functional groups, such as the alkyl amine of lysine, can neutralize the negative charge that accumulates as five electronegative oxygen atoms transiently form bonds with the phosphorus atom in the transition state (BOX 2). The IMIDAZOLE side chain of histidine ionizes in the neutral pH range, and it can therefore function to

TRANSITION-STATE THEORY
A general chemical theory whereby the trajectory of a chemical reaction proceeds from the starting reagents through a high-energy, short-lived transition state towards the products.

GENERAL ACID OR BASE
A proton acceptor or a proton donor that is not the solvent.

either accept a proton from the 2′-hydroxyl nucleophile or donate a proton to the oxyanion leaving group at neutral pH.

Although the biochemical and structural features of ribonucleotides make them well suited to the storage and transmission of genetic information through complementary base pairing, they are not particularly adept at catalytic chemistry. Ionization of the nucleotide bases and the ribose–phosphate backbone occurs at high or low pH (BOX 3), which makes it difficult for nucleotide bases to participate in general acid or base catalysis at neutral pH. At neutral pH, no positively-charged RNA functional groups are expected to be available to function as LEWIS ACIDS to activate a nucleophile, or to stabilize an electronegative transition state or an oxyanion leaving group.

Box 1 | **The reactions of self-cleaving and self-splicing ribozymes**

Self-cleaving and self-splicing ribozymes catalyse two types of phosphodiester-cleavage reaction. Self-cleaving RNAs catalyse a reversible cleavage reaction in which the 2′ hydroxyl is the attacking nucleophile (see figure part a, blue) and the bridging 5′ oxygen (see figure part a, red) is the leaving group. Phosphodiester-cleavage reactions that are mediated by ribonuclease (RNase) P and self-splicing introns involve the S_N2-type in-line attack of an exogenous nucleophile on phosphorus. The 3′-hydroxyl group of exogenous guanosine and the 2′-hydroxyl group of an adenosine in the intron are the attacking nucleophiles in the first steps of group-I and group-II self-splicing, respectively, whereas water is the attacking nucleophile during the RNase-P-mediated cleavage of precursor tRNA (the three possible nucleophiles are represented by ROH in the figure part b, and the oxygen nucleophile is highlighted in blue). The bridging 3′ oxygen (see figure part b, red) is the leaving group, and the new 3′ end of the 5′ exon becomes the attacking nucleophile during the second step of splicing.

Both types of phosphodiester-cleavage reaction proceed with an inversion of the stereochemical configuration of the nonbridging oxygen atoms that are bound to the phosphorus that is undergoing attack. This implies an S_N2-type in-line attack mechanism with a trigonal bipyramidal transition state, or intermediate, in which five electronegative oxygens form transient bonds with phosphorus (see figure, yellow shading). N–1 and N+1 are the nucleotide bases on the 5′ and 3′ sides of the reactive phosphodiester, respectively. The symbol ‡ indicates the transition states, and (H) represents hydrogens for which it is not clear whether, or how closely, they are associated with the oxygens.

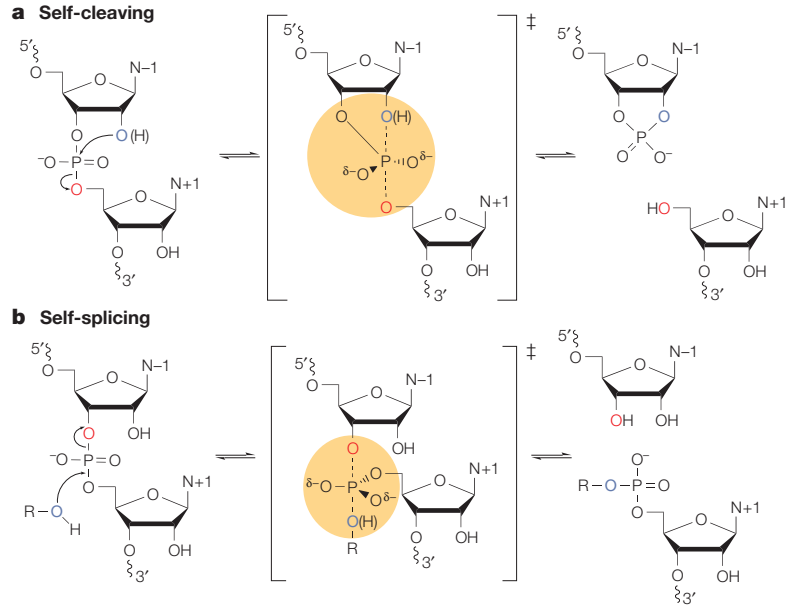

Virtually all ribozyme reactions are stimulated by divalent cations and, as recently as 1997, these catalytic reactions were all thought to function exclusively through the use of metal-cation cofactors. Protein metalloenzymes can catalyse similar reactions to those catalysed by ribozymes, and divalent metal-cation cofactors seemed to offer the chemical versatility that RNA functional groups lack[25] (BOX 4). Metal cations could stabilize oxyanion leaving groups, or stabilize the negative charge that develops in transition states. Metal-bound water could mediate general acid–base catalysis by donating protons to oxyanion leaving groups or by accepting protons from nucleophilic oxygens. Finally, the binding of metal ligands could align ribose and phosphate oxygens appropriately for an S_N2-type attack. However, metal cations are also required to neutralize the phosphodiester-backbone charge, and virtually all RNAs require counterions for assembly. Care was therefore needed to distinguish between nonspecific cation interactions that stabilize functional ribozyme structures and specific metal interactions that contribute directly to catalysis (BOX 4).

In this review, we discuss the mechanisms that are used by the small self-cleaving ribozymes, the group-I introns and the ribosome. All of these systems have been extensively studied by both mechanistic-enzymology and structural-biology approaches, and a number of common themes have emerged from this extensive body of work.

Small self-cleaving ribozymes

Hepatitis ribozyme catalysis of RNA cleavage. The ribozymes of HDV catalyse a self-cleavage reaction that generates products with 5′-hydroxyl and 2′–3′-cyclic-phosphate termini (BOX 1) and that is required for the processing of viral RNA replication intermediates[26]. Both the genomic and antigenomic strands of the circular viral RNA genome harbour self-cleaving ribozymes with virtually the same secondary structures. The 2.3-Å-resolution crystal structure of the 3′ product of self-cleavage by the genomic HDV ribozyme provided an early glimpse into the active site of an RNA enzyme[13,27] (FIG. 1a). The correlation that was found between the effects of functional-group modifications on activity and the interactions in the crystal structure indicated that the structure reflected a functional conformation[26].

The 5′ hydroxyl of the G1 nucleotide base, which forms part of the reactive phosphodiester in the pre-cleaved RNA, sits deep in a solvent-inaccessible cleft (FIG. 1a). Confounding the conventional wisdom that all ribozymes require divalent metal-ion cofactors, the structure showed no divalent metal near the terminal 5′ hydroxyl. Instead, the N3 of the cytosine base at position 75 (C75) is located within 2.7 Å of the 5′ oxygen (FIG. 1b). This structure, together with biochemical evidence that other self-cleaving RNAs remained functional in the absence of divalent metal cations[28–31], raised the intriguing possibility that active-site nucleotide bases participate directly in catalytic chemistry.

Box 2 | Concerted general acid–base catalysis by ribonuclease A

Ribonuclease (RNase) A is a protein enzyme that catalyses the same chemical reaction as self-cleaving RNAs. RNase A provides a textbook example of concerted general acid–base catalysis[90]. Residue His12, in its unprotonated form, functions as a general base catalyst to remove a proton from the attacking 2′-oxygen nucleophile, whereas His119, in its protonated form, functions as a general acid catalyst to protonate the 5′-oxygen leaving group. As shown in the figure, a hydrogen-bonding interaction between the positively charged ε-amino group of Lys41 and the nonbridging phosphoryl oxygen provides electrostatic stabilization to the transition state (represented by ‡).

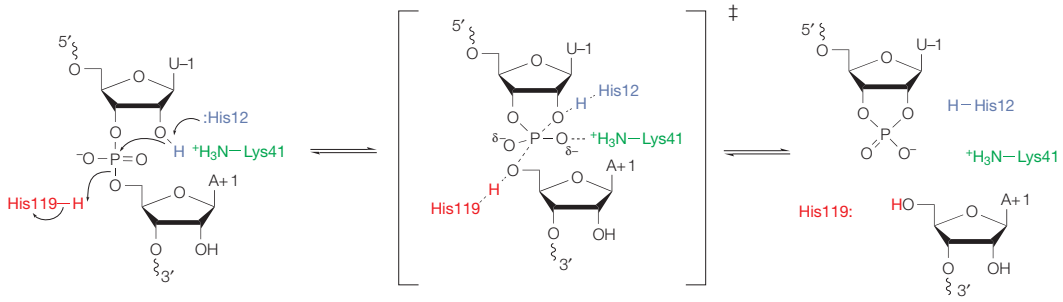

The functional groups on the nucleotide bases could accept or donate the protons that must be transferred during the course of the cleavage reaction.

The role of ionizable groups in catalysis can be analysed by studying the pH dependence of the reaction rate. The cleavage activity of the HDV ribozyme has a bell-shaped pH-RATE PROFILE, which provides evidence that the activity depends on the protonation state of two functional groups that ionize with apparent pK_a values that are close to 6.5 and 9 (REF. 32). Neither of these apparent pK_a values matches the pK_a value for cytidine ionization in solution, which is 4.2 (BOX 3). However, C75 might have a different ionization equilibrium in the active site. These considerations led to the model that C75 ionizes near pH 6.5 and, in its deprotonated form, functions as a general base catalyst to accept a proton from the 2′ oxygen, which activates this oxygen for a nucleophilic attack on the phosphorus[13,32] (FIG. 1c).

Subsequent NMR studies did not find direct evidence for a shifted pK_a of ~6.5 for C75 (REF. 33). However, ribozyme variants with C75 modifications showed changes in the pH dependence of cleavage rates that correlate with the pK_a of the variant nucleotide base[32,34]. For example, substituting adenine for the active-site cytosine changes the apparent pK_a of the reaction by a value that corresponds to the difference between the intrinsic pK_a values of cytosine N3 and adenine N1 (REFS 32,35; BOX 3). Exogenous cytosine, imidazole and nucleotide-base analogues in solution can rescue the activity of HDV ribozyme variants that lack C75, presumably by using the same mechanism as the missing cytosine[32,36]. Chemical rescue experiments with a series of imidazole analogues showed that the pH dependence of the rescue reaction correlated with the pK_a of the analogue. Importantly, the rate of the rescue reaction also correlated with the intrinsic basicity of the analogue, as well as with pH-dependent changes in the concentration of protonated and unprotonated analogue species[36]. This correlation with base strength would be expected if the rescuing analogue participates directly in proton transfer in the transition state[37]. Taken together, these experiments provide strong evidence that the cytosine mediates proton transfer in the catalytic mechanism of the HDV ribozyme.

However, interpreting the pH-rate profiles in terms of the specific ionizations that are responsible for changes in activity is complicated by the principle of KINETIC EQUIVALENCE[38]. Ambiguity arises from the fact that a mechanism that includes a general base (or general acid) and a mechanism that includes the combination of a general acid (or base) and a hydroxide ion (or a proton) both give equivalent rate equations. Accordingly, the same pH dependence is consistent with a second model, in which cytosine is a general acid, and a solvated hydroxide ion or a different base catalyst activates the 2′-oxygen nucleophile[26,35,36] (FIG. 1d). The hypothesis that C75 functions as a general acid catalyst is consistent with the location of C75 near the 5′-oxygen leaving group[13]. Of course, the 2′-oxygen nucleophile was missing in the structure of the 3′-cleavage-product RNA, so the proximity of C75 to the nucleophilic oxygen was unknown. Support for the second model came from the observation that the pH dependence of the activity varied with the divalent-metal-ion concentration, which indicated that the ionization of metal-bound water might contribute to the pH dependence[35,36,39]. These results were consistent with the idea that either hydroxide or a solvated metal hydroxide accepts a proton from the 2′ hydroxyl to activate the nucleophile, and that cytosine, in its protonated form, functions as a general acid catalyst to protonate the leaving group.

Crystal structures were solved recently for full-length HDV ribozyme RNAs in which the cleavage activity was blocked by a C75U mutation[14] (FIG. 1b). The uncleaved RNAs showed striking differences in the organization of the active site, compared with the cleaved RNA. The large distance between N3 of U75 and the 5′ oxygen in the uncleaved RNA indicates that the hydrogen bond between C75 and the leaving group in the cleaved RNA is absent in the C75U mutant. In

IMIDAZOLE
A small heterocyclic compound that contains two nitrogen atoms in a five-membered ring. Imidazole has chemical groups that can serve as a general acid or a general base in catalysis. The amino acid histidine has an imidazole group as its side chain.

LEWIS ACID
Any functional group or chemical that can interact with unpaired electrons.

pH-RATE PROFILE
The measurement of a reaction rate as a function of varying pH values, which can be an indicator of the presence of acid or base catalysis.

KINETIC EQUIVALENCE
The principle that underlies the fact that it is often not possible to determine if either acid- or base-catalytic mechanisms are operative from the pH dependence of a reaction rate. This is because different reaction mechanisms can give rise to identical pH-rate profiles that reflect different, but kinetically equivalent, rate equations.

Box 3 | **Ribonucleotides and acid–base catalysis**

In order to be effective at transferring protons, a general acid or base catalyst has to meet two criteria. First, a general acid or base catalyst has to be available in the appropriate ionization state — that is, a general acid catalyst has to have a proton available to donate and a general base catalyst has to have a deprotonated site available to accept a proton. Second, a general acid or base catalyst must be acidic or basic enough to donate or accept protons readily. In solution, ribonucleotide functional groups have ionization equilibria that are far outside the neutral pH range — the dissociation constant of an acid, the pK_a, is the pH at which it is half dissociated or ionized[92–94]. So, with pK_a values that are 4.2 or lower for cytidine, adenosine and guanosine, and 9.2 for uridine and guanosine (see figure), only a small fraction of these nucleotide bases would be in the right ionization state to accept protons from oxygen nucleophiles or to donate protons to oxyanion leaving groups at neutral pH. However, the ionization equilibria of nucleotide bases might vary owing to the proximity of charged phosphate groups or cations. For further information on the potential role of nucleotide-base ionization in catalytic chemistry, see REFS 52,95,96**.**

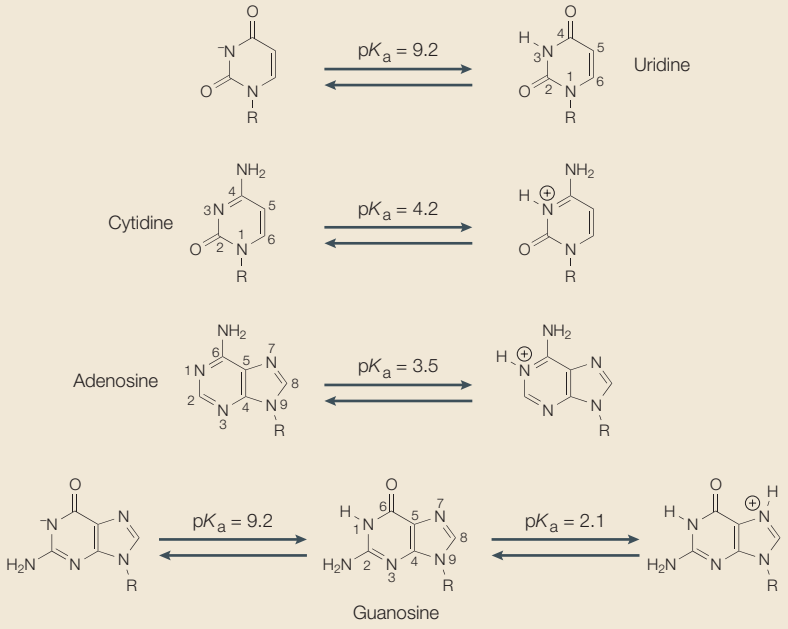

contrast to the cleavage product, in which no metal ions were found in the active site, a solvated metal ion is present near the 5′-oxygen leaving group of G1 in the uncleaved RNA. The same metal cation could not interact with the 2′-oxygen nucleophile without a conformational rearrangement, which argues against a role for such a cation in activating the nucleophile. So, the uncleaved RNA structure supports a model in which the solvated metal ion carries out general acid catalysis by protonating the 5′-oxyanion leaving group, whereas cytosine, in its unprotonated form, functions as a general base catalyst by deprotonating the 2′-oxygen nucleophile[14] (FIG. 1c). Further biochemical and structural evidence will be needed to establish whether the metal identified in the structure of the C75U mutant also occupies the active site of a functional ribozyme.

Hairpin ribozyme catalysis of RNA cleavage. The hairpin ribozyme catalyses the same reversible self-cleavage reaction as the HDV ribozymes (BOX 1) to process intermediates in the ROLLING-CIRCLE REPLICATION of PLANT SATELLITE RNAs[40]. A minimal hairpin ribozyme consists of two helix–loop–helix elements (domains A and B) that bend at the interdomain junction (FIG. 2a). Minimal hairpin ribozymes partition almost equally between a functional structure that allows the nucleotides in loops A and B to assemble the active site and an extended, nonfunctional conformation. Most of the disabling modifications of minimal ribozymes shift the equilibrium further towards the nonfunctional conformation, which makes it difficult to distinguish whether modifications that interfere with activity do so by disrupting structure and/or catalysis[41–43]. In viral satellite RNAs, the A and B domains comprise two arms of a four-way helical junction[44] (FIG. 2a). Restoring this natural junction stabilizes the docked structure, and ribozymes with a four-way junction retain activity despite unfavourable reaction conditions and destabilizing modifications[42,43,45–47]. The discovery of the stabilizing effect of the natural four-way junction made it possible to examine the effects of nucleotide modifications on catalysis in the context of a functional ribozyme structure.

Structures have been solved for hairpin ribozyme complexes with: a substrate analogue in which the 2′-hydroxyl nucleophile of adenosine at the –1 position (A–1) was blocked by a 2′-*O*-methyl group modification; a vanadate mimic of the trigonal bipyramidal transition state; and a cleavage-product RNA[15,16,48] (FIG. 2b). These structures correlate well with each other and with the functional consequences of the nucleotide modifications[49,50]. The crystal structures show the reactive phosphodiester in a conformation that is consistent with the in-line S_N2-type nucleophilic attack mechanism that had been inferred from reaction stereochemistry[51] (BOX 1). Consistent with biochemical data that show that hairpin ribozymes retain full function in the absence of divalent metal ions[28–31], no metal ions were seen in the active site.

The structures of the substrate analogue and vanadate complexes place the G8 and A38 nucleotide bases close to the reactive phosphate[15,16] (FIG. 2b). The N1 ring nitrogen of G8 is within hydrogen-bonding distance of the 2′ oxygen of A–1, which carries out the nucleophilic attack during cleavage and is the leaving group during ligation. The N2 exocyclic amine of G8 interacts with a nonbridging phosphoryl oxygen. The exocyclic amine of A38 interacts with the other nonbridging phosphoryl oxygen in the transition-state and cleavage-product structures, and its N1 ring nitrogen is near the 5′ oxygen of G+1, which carries out the nucleophilic attack during ligation and is the leaving group during cleavage.

The similarity between the active site of the hairpin ribozyme and RNase A (BOX 2) indicated that the two enzymes might use analogous catalytic mechanisms[15,52]. In a general acid–base model for the catalytic mechanism of the hairpin ribozyme, G8 would function as a general base to activate the 2′-oxygen nucleophile and A38 would function as a general acid to donate a proton to the 5′-oxygen leaving group during cleavage. However, adenine and guanine seem

ROLLING-CIRCLE REPLICATION
A replication mechanism commonly used by virus-associated RNAs, whereby a circular DNA or RNA template is continuously replicated around a circle to make a concatenated linear polymer of genomic copies. Self-cleaving ribozymes are often responsible for the cleavage of monomeric genomic RNAs from the linear polymeric strand, and for the rejoining of the monomeric RNA termini to form circular templates for subsequent rounds of replication.

PLANT SATELLITE RNA
An RNA that is associated with plant viruses and that does not itself contain any functional open reading frames.

ABASIC
Lacking a nucleotide base, which can occur, for example, when a nucleotide is substituted with a linker that maintains the ribose–phosphate backbone but has a hydrogen atom in place of the nucleotide base.

PURINE
An aromatic, heterocyclic base that consists of a six-membered pyrimidine ring fused to a five-membered imidazole. Adenine and guanine are the most common purines that are joined to ribose in the ribonucleotide building blocks of RNA.

PYRIMIDINE
An aromatic, heterocyclic base that contains two nitrogen atoms in a six-membered ring. Uracil and cytosine are the most common pyrimidines that are joined to ribose in the ribonucleotide building blocks of RNA.

THIOPHILIC
Attracted to sulphur.

to be unsuitable general acid–base catalysts, unless their ionization equilibria change in the active site (BOX 3). Nevertheless, minimal hairpin ribozymes show a shallow, bell-shaped pH-rate profile, which is consistent with the idea that their activity depends on the ionization of two functional groups, one with a very high pK_a value and one with a very low pK_a value, such as those characteristic of the N1 positions of guanosine and adenosine, respectively[29,40]. Furthermore, it can be argued that nucleotide bases could carry out reasonably efficient general acid–base catalysis , even with unaltered ionization equilibria, to achieve the catalytic rate accelerations that are typical of RNA enzymes[52].

The interpretation of pH-rate profiles for RNA enzymes (particularly minimal ribozymes) is further complicated by the fact that nucleotide-base ionization can destabilize functional RNA structures at pH extremes. The stable four-way junction form of the ribozyme does not show the same bell-shaped pH dependence as the unstable minimal ribozymes. Instead, the activity increases with increasing pH, and pH-rate profiles indicate that the catalytic activity depends on the ionization state of a functional group with an apparent pK_a value of ~6 (REFS 53,54). The loss of G8 significantly inhibits catalysis, as would be expected for an important active-site nucleotide base[54,55], but variants that lack G8 and unmodified ribozymes show the same apparent pK_a value of ~6 (REF. 54), which indicates that a change in the fraction of unprotonated G8 does not account for the pH dependence of the activity. By contrast, the loss of A38 does eliminate the change in activity near a pH of 6, which is characteristic of unmodified ribozymes[56]. This indicates that A38, and not G8, is associated with an ionization event that affects the catalytic activity either directly or indirectly. These data argue against the general acid–base model in which deprotonated G8 accepts a proton from the 2′-oxygen nucleophile.

Similar to the imidazole rescue of mutant HDV ribozymes[32], base analogues in solution can restore the activity of hairpin ribozymes with ABASIC substitutions of G8 and A38 (REFS 54–56). An abasic substitution maintains the continuity of the phosphodiester backbone but replaces the nucleotide base with hydrogen, which presumably leaves a solvent-filled cavity in the active site. A broad survey of heterocyclic amines showed that the minimal common element that is required for the rescue of abasic variants that lack G8 or A38 is an amidine — that is, an amino group in the α-position to a ring nitrogen. The same element is common to the Watson–Crick hydrogen-bonding faces of adenine and guanine, indicating that rescue occurs through the specific binding of an exogenous base in a cavity that was left by the abasic substitution.

The pH dependence of the rescue of an abasic ribozyme that lacks G8 varies according to the identity of the exogenous nucleobase in a way that indicates the rescue requires the protonation of the N1 position of PURINES or the N3 position of PYRIMIDINES[54,55]. A requirement for the protonation of N1 of G8 was also inferred from changes in the pH-rate profiles that accompany covalent modifications at this position[53]. These data indicate that interactions with protonated G8 stabilize the negative charge that develops in the transition state (FIG. 2c,d). Substitutions of A38 with nucleotide analogues alter pH-rate profiles in ways that implicate A38 ionization in catalysis[56]. The pH dependence of activity is consistent with two models in which the functional form of A38 is either protonated or unprotonated (FIG. 2c,d). In the first model, protonated A38 would function as a general acid by donating a proton to the 5′ oxygen, acting in concert with a hydroxide ion that activates the 2′-oxygen nucleophile during cleavage, and unprotonated A38 would function as a general base to activate the 5′-oxygen nucleophile during ligation (FIG. 2c). In the second model, unprotonated A38 accepts a hydrogen bond from the 5′-hydroxyl nucleophile during ligation, and accepts a hydrogen bond from a protonated bridging 5′ oxygen during cleavage, which provides electrostatic stabilization to the developing negative charge (FIG. 2d). In both models, a hydrogen bond forms between N1 of adenine and the 5′ oxygen, which is consistent with the active-site structure (FIG. 2b). The amidine group of G8, in its protonated form, donates hydrogen bonds to the 2′ and phosphoryl oxygens to provide electrostatic stabilization as a negative charge develops in the transition state.

Box 4 | Divalent metal-cation cofactors and RNA enzymes

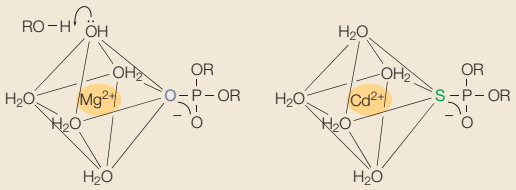

Divalent metal cations, such as Mg^{2+}, can interact with RNAs through inner sphere (direct) coordination to phosphate and ribose oxygens. In this way, they can activate nucleophilic oxygens during oxygen–phosphorus bond formation or stabilize oxyanion leaving groups during oxygen–phosphorus bond breakage, and counter negative charges that develop on nonbridging oxygens in transition states. Diffusely associated metal cations also interact nonspecifically with RNAs and facilitate the assembly of functional structures by neutralizing the phosphate charge (for reviews, see REFS 97,98). Mg^{2+} is a particularly effective counterion for stabilizing RNA structures because of its small size and high charge density.

Metal-cation specificity-switch experiments are used to distinguish metal cations that stabilize RNA structures from those that participate directly in catalysis. A specificity switch reflects the change in affinity for 'hard' and 'soft' metal cations that accompanies the substitution of specific phosphate or ribose oxygens with sulphur or nitrogen. Mg^{2+} is a hard metal ion that interacts efficiently with oxygen, which is a hard ligand (see figure, left panel), but Mg^{2+} interacts poorly with soft ligands, such as sulphur or nitrogen. Soft metal cations such as Mn^{2+} or Cd^{2+} interact efficiently with sulphur or nitrogen ligands (see figure, right panel)[99]. When the interaction of Mg^{2+} with a particular oxygen ligand participates in catalysis, substituting sulphur for the oxygen ligand changes the metal-cation dependence of the reaction. Activity that is lost in reactions with Mg^{2+} is restored by THIOPHILIC Mn^{2+} or Cd^{2+} cations. Metal-cation rescue experiments can be subject to artefacts owing to differences in the size, electronegativity and polarizability of sulphur and oxygen, as well as differences in their affinity for hard and soft metals[100]. Sulphur substitutions can also interfere with interactions other than metal binding[101].

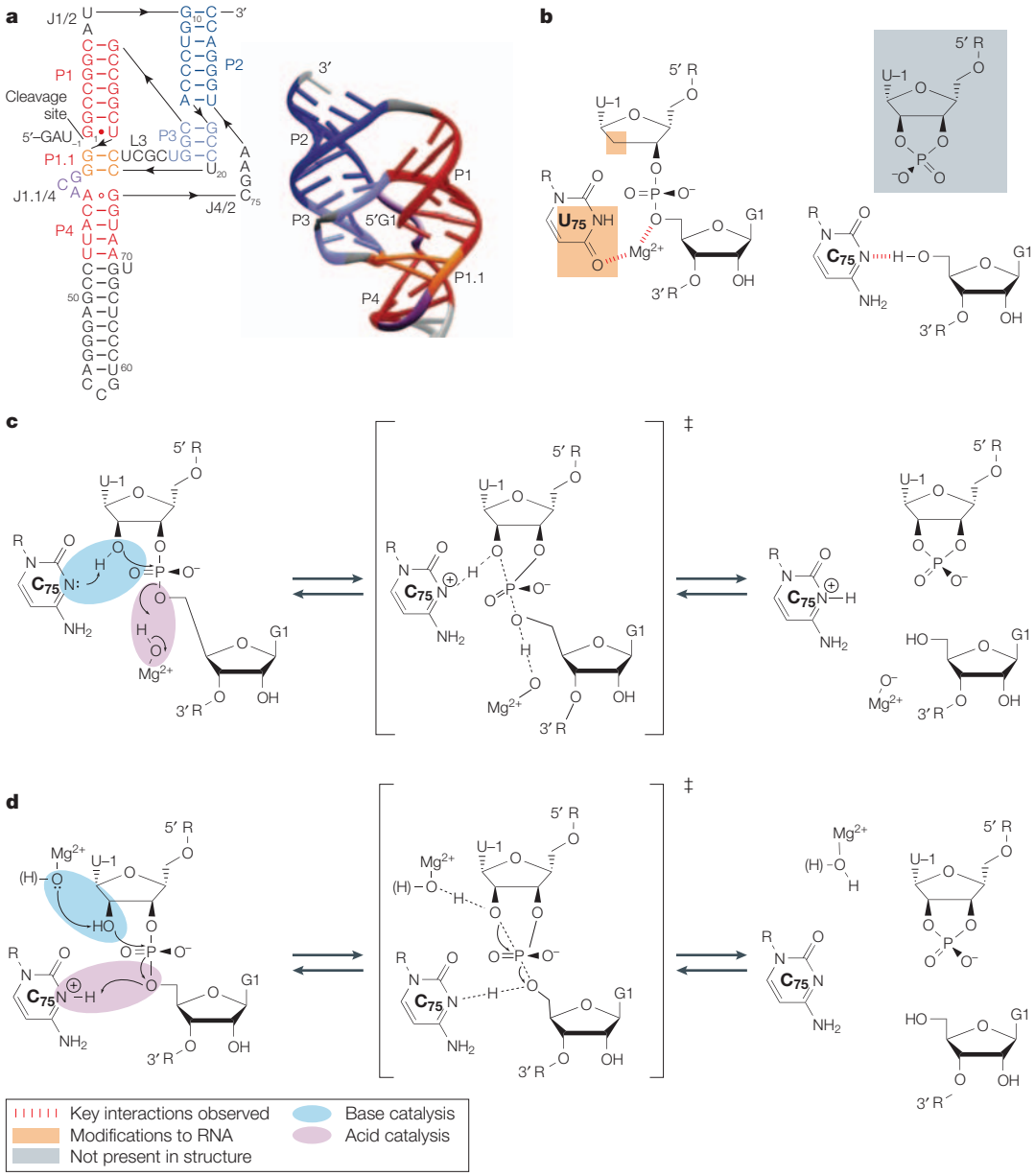

Figure 1 | **Hepatitis delta virus ribozyme structure and mechanism. a** | The secondary structure of the hepatitis delta virus (HDV) ribozyme[26] and the cleavage product ribbon model[13]. P and L indicate base-paired and loop regions, respectively, and J refers to joining regions. The 5′-terminal residue, G1, is in a solvent-inaccessible cleft. The filled red circle represents a 'wobble' base pair (as opposed to a canonical Watson–Crick pair), whereas the open red circle represents a non-canonical purine–purine pair, which is wider than a Watson–Crick pair and opens the minor groove. **b** | Key interactions in the HDV ribozyme active site as seen in two crystal structures. The diagram on the left represents the complex between the substrate and a ribozyme that had been inactivated by C75U and deoxy-U–1 substitutions (the 'substrate complex'). Mg^{2+} contacts the 5′-oxygen group of G1 and the 4-carbonyl group of U75. The diagram on the right represents the complex between the active HDV ribozyme and the cleaved product (the 'product complex'), with U–1 cleaved from the structure. The N3 atom of C75 forms a hydrogen bond with the 5′ hydroxyl (OH) of G1. **c** | General acid–base model for HDV ribozyme cleavage. The N1 group of C75 could function as a general base to remove the 2′-OH proton, and a Mg^{2+}-coordinated water molecule (which is shown deprotonated in the figure) could serve as the general acid to protonate the 5′-OH leaving group. **d** | Alternative general acid-specific base catalysis model. A weakly associated hydroxide (a SPECIFIC BASE) or Mg^{2+}-coordinated hydroxide could remove the proton from the 2′-OH group, and the protonated form of C75 could serve as the general acid to protonate the 5′-OH leaving group. The protonation state of the Mg^{2+}-coordinated molecule is unknown (highlighted by (H)), and the base could be either a coordinated water molecule or a hydroxide ion). The two mechanisms in **c** and **d** are kinetically indistinguishable, and it is possible that C75 could serve as either a general acid or a general base catalyst. R indicates the nucleotides flanking the U–1 and G1 nucleotides that form the reactive phosphodiester, and the symbol ‡ indicates the transition states. The left panel of part **a** is modified with permission from REF. 26 © (2002) Annual Reviews. The right panel of part **a** is reproduced with permission from *Nature* REF. 13 © (1998) Macmillan Magazines Ltd.

SPECIFIC ACID OR BASE
Solvent acid or base species, which, for water, are H^+ and OH^-.

Hammerhead ribozyme catalysis of RNA cleavage. The hammerhead ribozyme was the first self-cleaving RNA to be discovered[57,58], the first ribozyme to be crystallized[6,7], and has been the focus of more studies than any other catalytic RNA. Even so, a complete understanding of its reaction mechanism remains elusive (for recent reviews, see REFS 10,59–62). Hammerhead and hairpin ribozymes are found in opposite strands of the same plant virus satellite RNAs, and they catalyse identical chemical reactions[51]. Nonetheless, the two ribozymes adopt different structures and have different biochemical features, including different pH and metal-cation dependencies and different proficiencies for catalysing RNA ligation[40].

A minimal hammerhead contains three base-paired helices (helices I, II, and II) around a core of conserved nucleotides (FIG. 3a). Nearly identical hammerhead crystal structures were determined for both an RNA–DNA hybrid[6] and an RNA complex with a 2′-*O*-methyl group at the cleavage site to block activity[7] (FIG. 3b). In both structures, the angle between the 2′-oxygen nucleophile and the 5′-oxygen–phosphorus bond is almost 90° away from the alignment that is necessary for an S_N2-type attack mechanism[63], which indicates that crystallization trapped the hammerhead in an inactive conformation. Mechanistic and X-ray studies fail to give a coherent picture of the active site, in that a number of nucleotide modifications that interfere with catalysis form no identifiable interactions in the structure[63]. Furthermore, quantitative metal-titration studies with modified hammerhead ribozymes that contain sulphur substitutions (BOX 4) indicate that the binding of a single divalent metal cation to the PRO-R_p nonbridging oxygens of both A9 in helix II and C17 at the cleavage site promotes activity, but the crystal structures show that these two ligands are 20 Å apart[64,65] (FIG. 3b). Crystal structures have also been solved for several modified hammerhead ribozymes under conditions that are designed to trap reaction intermediates[8,9,11], but these structures do not resolve all of the structure–function discrepancies that were noted in the original structures. Even so, biophysical and functional studies indicate that these crystal structures reflect the dominant conformation in solution and are not artefacts of crystallization (for recent reviews, see REFS 61,62). The formation of the transition state therefore evidently requires a significant conformational rearrangement, which limits the mechanistic insights that can be gained from inspecting these structures.

The discovery that interactions between loops I and II draw helices I and II — the arms of the Y structure — close together is likely to be important in this respect[66,67]. Similar to the enhanced stability of four-way junction hairpin ribozymes, hammerhead ribozymes that are stabilized by this tertiary interaction are functional under unfavourable reaction conditions[68–70]. Hammerhead ribozymes with these peripheral interactions might prove more tractable than minimal hammerheads to mechanistic and structural studies. Further characterization of stable hammerhead variants might well reveal that some of the biochemical features that seem to distinguish the hammerhead reaction mechanism from the hairpin and HDV ribozyme reaction mechanisms might actually reflect a dominant contribution of folding steps to the hammerhead reaction pathway.

PRO-R_p AND PRO-S_p
The chemical terms that specify the two stereochemically distinct nonbridging oxygen atoms of a phosphodiester.

Group-I intron catalysis of self-splicing

Group-I introns are a broad class of self-splicing RNAs with a well-defined core consensus sequence, which consists of elements P4–P6 and P3–P9 (FIG. 4a). Group-I intron self-splicing occurs in two steps[71] (FIG. 4b). The first step is the attack of the 3′-oxygen nucleophile of an exogenous guanosine cofactor on the 5′-exon–intron junction, which cleaves the junction and adds guanosine to the 5′ end of the intron. 3′-splice-site cleavage and exon ligation occurs in the second step, in which the 3′ oxygen of the 5′ exon carries out nucleophilic attack on the 3′-terminal guanosine of the intron. Chemically, the second step is equivalent to the reverse of the first step. The chemical reactions that group-I self-splicing introns catalyse are also catalysed by protein enzymes, such as the 3′–5′-exonuclease domain of DNA polymerase I, alkaline phosphatase and several restriction enzymes.

Structural and biochemical studies support a two-metal model of the catalytic mechanism for these protein enzymes (see REFS 25,72 and references therein). In this model, one metal cation, M_A, interacts with the leaving group oxyanion to neutralize the negative charge that develops during breakage of the oxygen–phosphorus bond, whereas another metal cation, M_B, activates the nucleophilic oxygen by withdrawing electrons (FIG. 4c). Interactions of the same two metal cations with nonbridging oxygens orientate the reactive groups for in-line nucleophilic attack and for displacement of the leaving group, and contribute electrostatic stabilization to the transition state.

Support for the idea that group-I introns undergo self-splicing through a variation of this two-metal mechanism[25] has come from metal-cation specificity-switch experiments[73]. These experiments are designed to identify catalytically important metal-cation interactions based on the different binding specificities of hard and soft metal cations for hard and soft ligands (BOX 4). Substituting sulphur for the 3′ oxygen at the 5′-exon–intron junction or for the 3′ oxygen of the exogenous guanosine nucleophile was shown to inhibit activity in reactions with the 'hard' Mg^{2+} cation, but not in reactions with more thiophilic Mn^{2+} or Cd^{2+} cations[74–78]. Rescue by thiophilic metal ions provides strong evidence for a direct interaction between the thiophilic metal cations and sulphur and, by inference, between Mg^{2+} and the corresponding nucleophilic and leaving group oxygens of the unmodified substrate (FIG. 4c). Interaction of a third metal cation, M_C, with the 2′ oxygen of the exogenous guanosine cofactor was inferred from the ability of thiophilic cations to rescue the inhibition that results from replacing the 2′ hydroxyl of guanosine with a 2′-amino group (REFS 75,79; FIG. 4c). Rescue at each site displayed a unique metal-ion concentration dependence, which provided evidence that

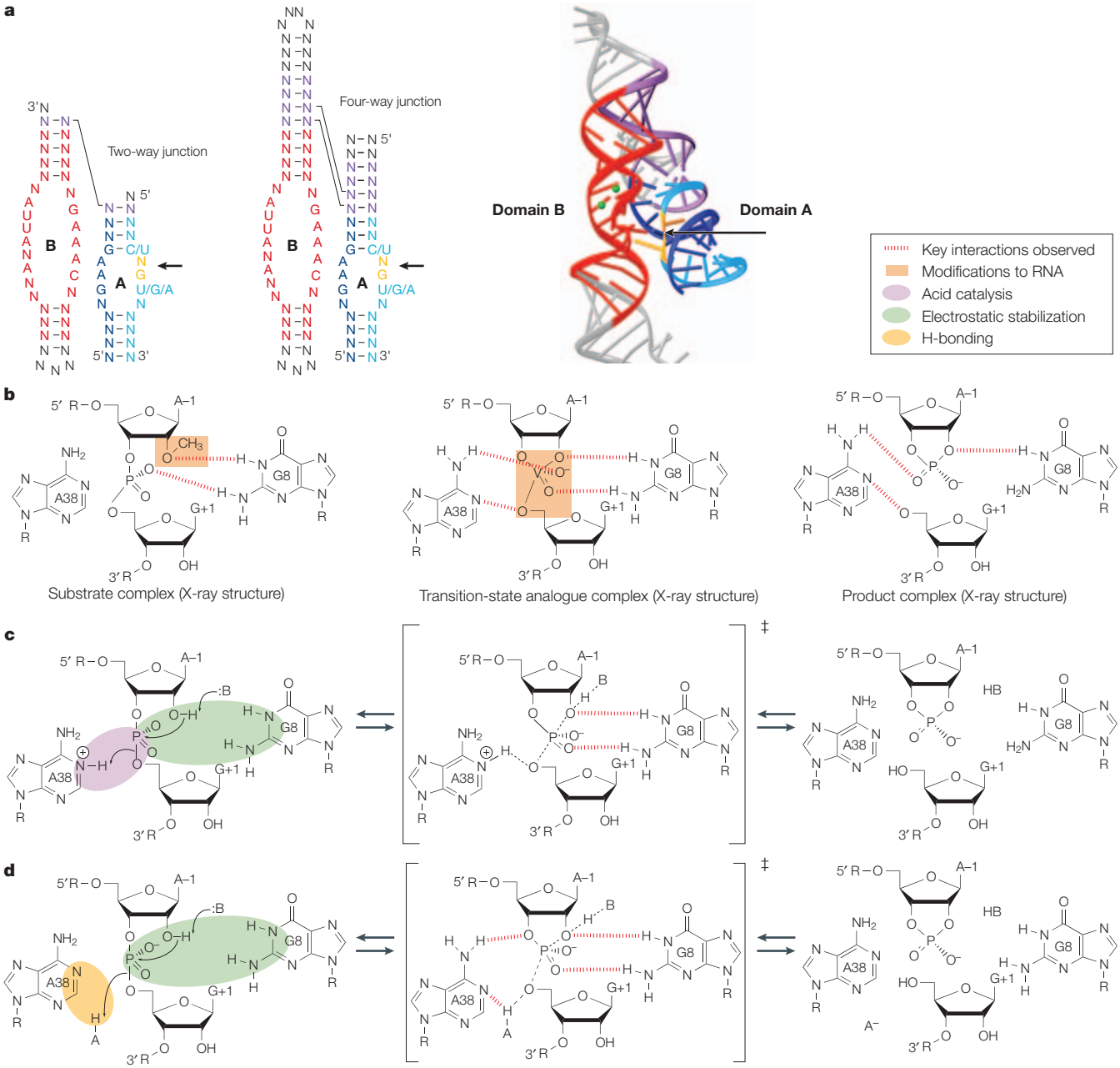

Figure 2 | **Hairpin ribozyme structure and mechanism. a** | Secondary structure diagram of the two-way junction and the four-way (natural) junction form of the hairpin ribozyme, and the crystal structure of the hairpin ribozyme complex with a noncleavable substrate analogue[15]. Arrows highlight the reactive phosphodiester. The colours highlight: G+1, A–1 and the reactive phosphodiester (yellow); domain A (blue); domain B (red); and the extra helices that form a four-way helical junction (purple). With respect to A–1, an adenosine is at this non-conserved (N) position in the natural hairpin ribozyme and the RNA used for crystallization. The green spheres represent two bound calcium ions. **b** | Interactions seen in three crystal structures of the hairpin ribozyme. The left panel shows the structure of the 'substrate complex' that is formed between the ribozyme and the substrate (the substrate had been modified to prevent cleavage). The G8 nucleotide base makes two hydrogen-bonding contacts — one with a phosphate oxygen and another with the 2′ oxygen. The middle panel shows the structure of the ribozyme complex with vanadate, which is a phosphate analogue that mimics the trigonal bipyrimidal transition state. In addition to the interactions with G8, interactions between A38 and the vanadate group are seen. The right panel shows the structure of the 'product complex', which is formed between the ribozyme and the cleaved product, and highlights interactions with A38 and G8. **c** | The proposed mechanism for hairpin ribozyme catalysis comprises general acid catalysis by the protonated form of A38 and the electrostatic stabilization of the transition state by G8. **d** | An alternative mechanism proposes that both A38 and G8 directly stabilize the transition state, but that specific acid and specific base catalysis mediate the required proton-transfer reactions. A–H is the acid catalyst that donates a proton to the 5′-oxygen leaving group during cleavage, whereas its unprotonated form, A^-, accepts a proton from the 5′-oxygen nucleophile during ligation. The symbol :B represents the base catalyst that accepts a proton to activate the 2′-oxygen nucleophile during cleavage, whereas HB, its protonated form, donates a proton to the 2′-oxygen leaving group during ligation. The symbol ‡ indicates the transition states. The right panel of part **a** is reproduced with permission from *Nature* REF. 15 © (2001) Macmillan Magazines Ltd.

three discrete metal ions with different binding affinities make individual contributions to catalysis[76]. Extension of this approach led to the conclusion that the metal ions that are associated with the 3′-oxygen leaving group (M_A) and the 2′ hydroxyl of guanosine (M_C) both also coordinate a nonbridging oxygen, whereas the metal ion that is associated with the 3′-oxygen nucleophile (M_B) does not[77,78]. The complete set of metal-cation interactions that have been inferred from cation specificity-switch experiments is shown in FIG. 4c.

The recent 3.1-Å structure of an *Azoarcus* spp. strain BH72 pre-tRNA intron provided the first opportunity to evaluate the three-metal model of group-I intron catalysis with a structural view of the active site[17,19] (FIG. 4d). Activity was blocked using 2′-deoxy substitutions of four 2′ hydroxyls in the active site. This structure represents the state of the intron after 5′-exon–intron cleavage, when it is poised to carry out intron–3′-exon cleavage and exon ligation in the second step of self-splicing. The 3′ hydroxyl of the 5′ exon is aligned for in-line nucleophilic attack at the 3′-terminal guanosine of the intron, which, again, emphasizes the crucial role of the active-site architecture in positioning and orienting the reactants. No direct interactions occur between the reactants and nucleotide-base functional groups, as were observed in the active sites of self-cleaving ribozymes. Instead, two metal-binding pockets are found on either side of the reactive phosphate (FIG. 4d). One pocket, which is comprised of five phosphate oxygens from three interconnected strands, is occupied by an Mg^{2+} cation. This Mg^{2+} cation, known as M_1, also interacts with the 3′ hydroxyl of the 5′ exon and a nonbridging oxygen of the reactive phosphate, which are the ligands that correspond well to those that were assigned to M_A in metal specificity-switch experiments. A K^+ cation, known as M_2, rather than the expected Mg^{2+} cation, occupies the second pocket, which is comprised of three nonbridging phosphate oxygens and two water molecules. The K^+ cation forms a water-mediated interaction with a nonbridging oxygen and lies near the expected location of the 2′ hydroxyl of guanosine that is missing in the construct used to obtain the structure. This indicates that M_2 might correspond to M_C, if the Mg^{2+} specificity was altered by the inactivating 2′-deoxy substitution. No evidence of a third metal cation that is analogous to M_B was found near the 3′ hydroxyl of the terminal guanosine.

Further insights into the self-splicing reaction pathway have come from a 3.8-Å structure of the *Tetrahymena thermophila* ribozyme, in which the 3′-terminal guanosine of the intron is bound in the active site, but in which the substrate RNA is missing[18], and also from a 3.8-Å structure of the bacteriophage Twort intron complex with a small exon cleavage product[20]. A single metal cation that is in a position intermediate to positions M_1 and M_2 was found in the *T. thermophila* ribozyme structure that lacks the intron–exon junction substrate RNA[18]. This metal

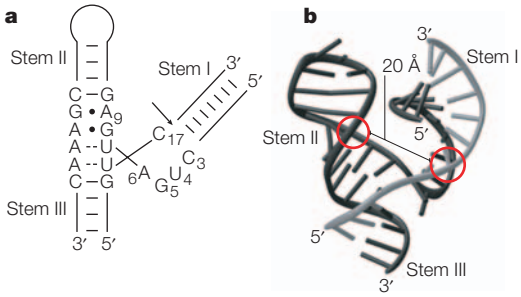

Figure 3 | **Hammerhead ribozyme structure. a** | The secondary structure of a hammerhead ribozyme[102]. Stems I, II and III are base-paired helices oriented in a Y shape around a core of conserved nucleotides. The arrow indicates the reactive phosphodiester. The black filled circles represent non-Watson–Crick purine–purine base pairs. Dashed lines indicate base pairs that form with just a single hydrogen bond. **b** | The crystal structure of a hammerhead ribozyme[102]. A9 (highlighted by the red circle on the left) and the cleavage site (right red circle) are located 20 Å apart in the structure, which is difficult to reconcile with mechanistic data indicating that these ligands are close enough to bind to the same metal cation. Part **a** was reproduced, and part **b** was modified, with permission from REF. 102 © (2000) Annual Reviews.

cation interacts with both the 2′ and 3′ hydroxyls of the terminal guanosine, and could correspond to either M_B or M_C. The bacteriophage Twort intron structure reveals details of 2′-hydroxyl interactions that are missing in the *Azoarcus* spp. BH72 structure, but it lacks the reactive phosphate. A comparison of the electron-density maps that are obtained in the presence and absence of Mn^{2+} identified a single divalent metal that is close to the 3′ hydroxyl at the 5′ splice site, which is consistent with its assignment as M_A, but no density that corresponded to M_B or M_C was seen.

Apart from differences that can be attributed to sequence differences and the presence or absence of substrate RNAs, the three group-I intron structures correlate well with each other and with most structure–function relationships that have been inferred from previous biochemical studies[17–20]. Despite this general consistency, the number and position of the metal cations that have been identified in these active-site structures do not correspond perfectly with the three-metal model inferred from metal-cation specificity-switch experiments (FIG. 4c). If the biochemical tabulation of active-site metals is accurate, and if these crystal structures represent functional intermediates along the reaction pathway, a conformational rearrangement would be required to accommodate three metal cations in the transition state.

The ribosomal catalysis of protein synthesis

The ribosome is a ribozyme that catalyses the formation of peptide bonds in protein synthesis. The chemistry of amide-bond formation through the attack of an amine nucleophile on an ester bond is distinct from the phosphate-group transfer reactions that are catalysed by other ribozymes. However, the catalytic requirements for transition-state stabilization are quite similar

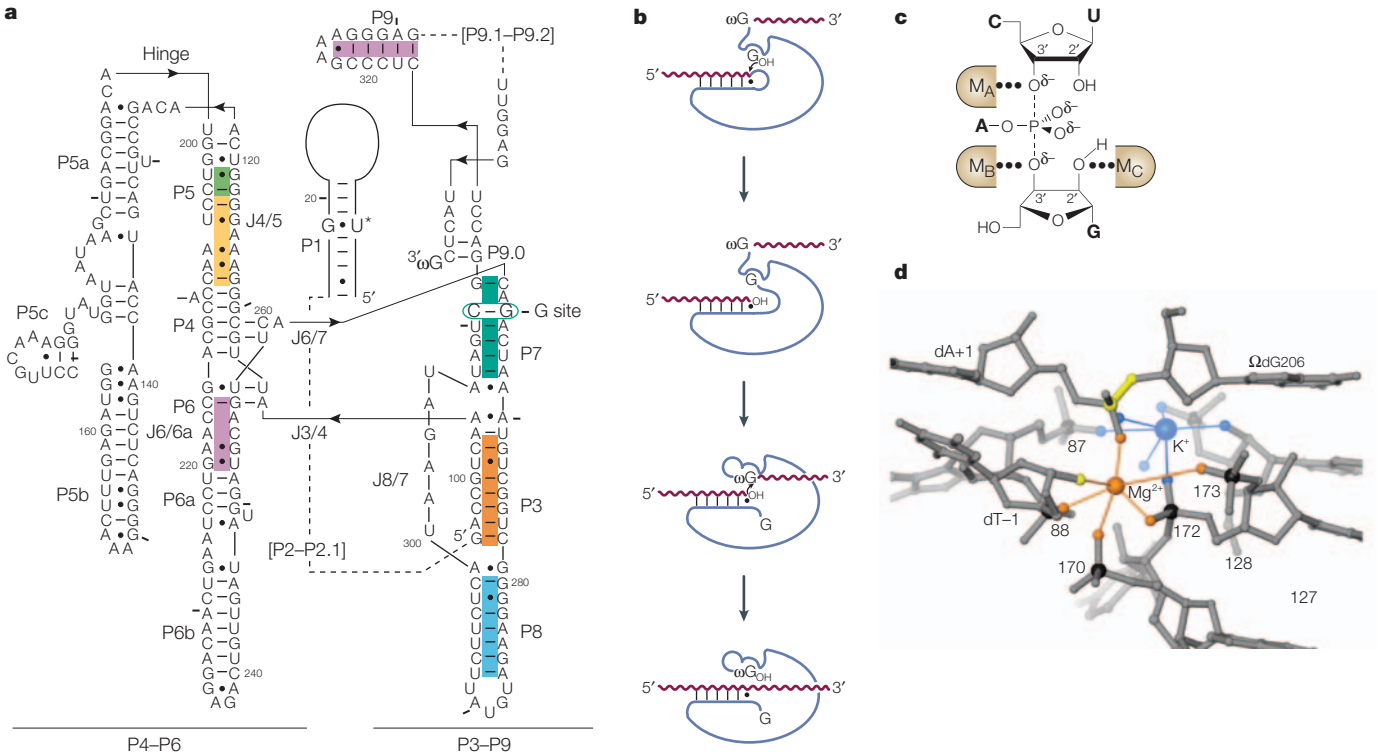

Figure 4 | **Group-I intron catalysis of self-splicing. a** | Secondary structure of the *Tetrahymena thermophila* group-I intron[103]. The conserved domains P4–P6 and P3–P9 are labelled, and the colours represent different helices. J represents joining regions between base-paired helices, and the * symbol indicates the 5′ splice site. The G site in P7 binds the exogenous guanosine cofactor. ωG is the 3′-terminal guanosine, and the dashed lines highlight nonconserved regions that have been omitted for clarity. The black filled circles represent non-Watson–Crick base pairs. **b** | The self-splicing pathway for group-I introns[18]. Binding of a guanosine nucleophile initiates the first step by attacking the 5′ splice site. A conformational change places the ωG group at the 3′ end of the intron into the guanosine-binding site, which sets up the second step of splicing. Attack of the 3′ hydroxyl (OH) of the 5′ exon results in ligation of the exons (shown in purple) and release of the intron (shown in blue). **c** | The three-metal model for catalysis of phosphoryl transfer reactions by the group-I intron[76]. In this model, one metal cation, M_A, interacts with the leaving group oxyanion to neutralize the negative charge that develops during breakage of the oxygen–phosphorus bond, whereas another metal cation, M_B, activates the nucleophilic oxygen by withdrawing electrons. A third metal cation, M_C, interacts with the 2′ oxygen of the exogenous guanosine cofactor. The black circles represent coordination of the oxygens by the metals. A is the adenosine at the 5′ end of the intron. **d** | The active site in the crystal structure of the group-I intron[17] showing the location of two metal ions, Mg^{2+} and K^+. dA+1 and dT–1 are the nucleotides outside the intron sequence. ΩdG206 is the 3′-terminal guanosine of the intron, although, in the crystal structure, it is a deoxyresidue. The colours show the atoms that coordinate K^+ (blue), the atoms that coordinate Mg^{2+} (orange), and the reactive bond and nucleophilic groups (yellow). Part **a** was modified with permission from REF. 103 © (1998) The American Association for the Advancement of Science. Part **b** was modified with permission from REF. 18 © (2004) Elsevier. Part **c** was modified with permission from REF. 76 © (1999) National Academy of Sciences, USA. Part **d** was reproduced with permission from *Nature* REF. 17 © (2004) Macmillan Magazines Ltd.

because both reactions involve nucleophilic attack at an electropositive centre and a developing negative charge in the transition state. In addition, both require base functionality to activate the nucleophile and acid functionality to protonate the leaving group (FIG. 5a).

Certainly, prior to the identification of catalytic RNAs, there was the expectation that the catalysis of peptide-bond formation would be carried out by ribosomal proteins. Although it was shown that most of the large subunit ribosomal proteins are dispensable for the formation of peptide bonds *in vitro*[80], it was not until the atomic resolution structure of the 50S subunit was solved that the unambiguous role for RNA as the catalytic functionality in protein synthesis was established. A crystal structure of the *Haloarcula marismortui* 50S subunit in complex with a synthetic transition-state analogue of the peptidyl-transferase intermediate showed that no protein atoms were located closer than 18 Å away from the reaction centre[3] (FIG. 5b). The ribosome active site — the peptidyl-transferase centre (FIG. 5c) — consists entirely of ribosomal RNA, and residue A2451 in *Escherichia coli* rRNA (A2486 in *H. marismortui* rRNA), in particular, makes hydrogen-bonding interactions with the proposed transition state (FIG. 5d). The structure, coupled with the observation that A2451 showed an unusual pK_a that had shifted into the neutral pH range[81], led to the reasonable proposal that A2451 functions as the general base during peptide-bond formation.

As has been the case for the other catalytic RNAs, interpreting the structural data and synthesizing the kinetic data into a mechanism of catalysis have proved

challenging. It was quickly shown that mutating A2451 did not abrogate the peptidyl-transferase reaction[82], and also that the altered pH-related chemical reactivity of A2451 was due to a conformational change in the active site[83]. Ultimately, the well-known pH dependence of peptide-bond formation could not be simply explained by inspecting the crystal structure.

Further insights into the mechanism of peptide-bond formation came from rapid kinetics experiments, which looked at a single turnover of the peptidyl-transferase reaction using P-SITE-bound peptidyl-tRNA and PUROMYCIN — which is a minimal antibiotic compound that mimics the 3′-acyl-adenosine residue on an A-SITE aminoacyl-tRNA — as the A-site substrate[84]. The essence of this work is that the ionization of a functional group contributes ~100-fold to the catalytic rate acceleration of peptide-bond formation. The observed pH-rate profile was consistent with a role for two titratable groups with different pK_a values, and one of these protonation sites was assigned to the amino-group of the puromycin model substrate[84]. The identity of the remaining ionizable group is unknown, although there are many candidate nucleotides in the peptidyl-transferase centre[85]. The overall rate acceleration for the chemical step of peptide-bond formation is ~100,000-fold. If 100-fold is attributable to acid–base catalysis, then ~1,000-fold is presumably attributable to other mechanisms that include the precise positioning of the reactive groups[84,86].

Recent biochemical evidence indicates that the 2′-hydroxyl group of the terminal nucleotide of the peptidyl-tRNA in the P site is the most crucial functional group in peptide-bond formation that has been identified so far[87]. The terminal 2′-hydroxyl group is immediately proximal to the 3′-amino-acyl bond, and is therefore extremely close to the transition state during peptide-bond formation. What is remarkable about this group is that it is located on the tRNA P-site substrate rather than on the ribosome itself. Modification of this group essentially abrogates peptide-bond formation on the ribosome. Although the terminal tRNA 2′-hydroxyl group in the P site is clearly crucial, its specific role in catalysis is not so clear. This group could serve as a general acid or base, or it could participate in forming the structure that activates the acid or base catalytic group.

Much of the detailed analysis of the mechanism of peptidyl-transfer activity by the ribosome has been carried out using the A-site analogue puromycin, which has allowed rapid kinetics to be measured in the absence of the relatively slow delivery of the A-site tRNA substrate by the translation elongation factor EF-Tu. Recently, it has been shown that mutation of the four conserved residues that are closest to the peptidyl-transferase reaction has dramatic effects on the puromycin model reaction, but little or no effect on reactions that use an intact A-site tRNA substrate[88]. Furthermore, these conserved nucleotides have an important role in peptide release, during which the peptidyl-tRNA acyl bond must be hydrolysed by a relatively poor water molecule nucleophile.

Again, the crystal structure of the ribosome gives profound structural insights into many aspects of ribosome function, but the details of catalysis remain elusive. The peptidyl-transferase active site is part of a larger complex active site that must allow significant structural rearrangements during translocation from one codon to the next, and during delivery and loading of the tRNA substrates. The conformational flexibility in this region further compounds the intrinsic difficulties of inferring mechanisms from kinetic data, a problem that arises in analyses of all the ribozymes. The ability to visualize the organization of the active site does permit hypotheses to be formed and tested using the tools of enzymology, and this is an active area of study. The picture is still murky, but the waters are clearing.

Concluding remarks

RNA enzymologists are learning that combining structural and mechanistic studies to deduce catalytic mechanisms is an iterative process. The general acid–base mechanism of RNase A catalysis was proposed 44 years ago, but remains a subject of active investigation and spirited debate to this day[89–91]. History indicates that RNA enzymologists are no more likely to get it right first time and, in fact, most of the initial mechanistic hypotheses for each ribozyme system have been significantly revised. To the extent that a crystal structure resembles the transition state, it can be invaluable for identifying functional groups that are candidates for participation in the catalytic chemistry. However, no crystal structure represents a true transition state, which is the highest energy, least probable structure along the reaction pathway that exists only on the timescale of bond vibration. Careful mechanistic studies remain necessary to confirm which groups mediate catalysis and how they do this. Of course, models of catalytic mechanisms that emerge from mechanistic studies must also pass the structural test — functional groups that carry out the catalytic chemistry have to interact physically with the reactants.

Compared with studies of protein enzymes, the application of conventional enzymological approaches to understanding ribozymes has turned out to be complicated because of the polyanionic nature of RNA. Changes in pH and ionic conditions can have dramatic effects on the kinetics of RNA folding and the stability of functional RNA structures. We now see that special care must be taken to distinguish between the direct effects of pH and metal cations on catalytic chemistry and indirect effects on the assembly and stability of RNA structures. Researchers in the field had expected RNA structures to be as insensitive to changes in pH across the neutral range as the ionization of nucleotides in solution. Indeed, the pH dependence of reaction kinetics was taken as evidence that the observed rates were monitoring catalytic chemistry and not a conformational change. The extent to which proximity to charged phosphates and cations can alter ionization equilibria is only now being explored, and the degree to which changes in pH can influence the stability of functional RNA structures has probably

P SITE
The site in the peptidyl-transferase centre of the ribosome that binds to the tRNA that is attached to the growing peptide chain.

PUROMYCIN
An antibiotic compound that inhibits protein synthesis and that binds to the ribosome as an analogue of aminoacyl-tRNA.

A SITE
The site in the peptidyl-transferase centre of the ribosome that binds the incoming aminoacyl-tRNA.

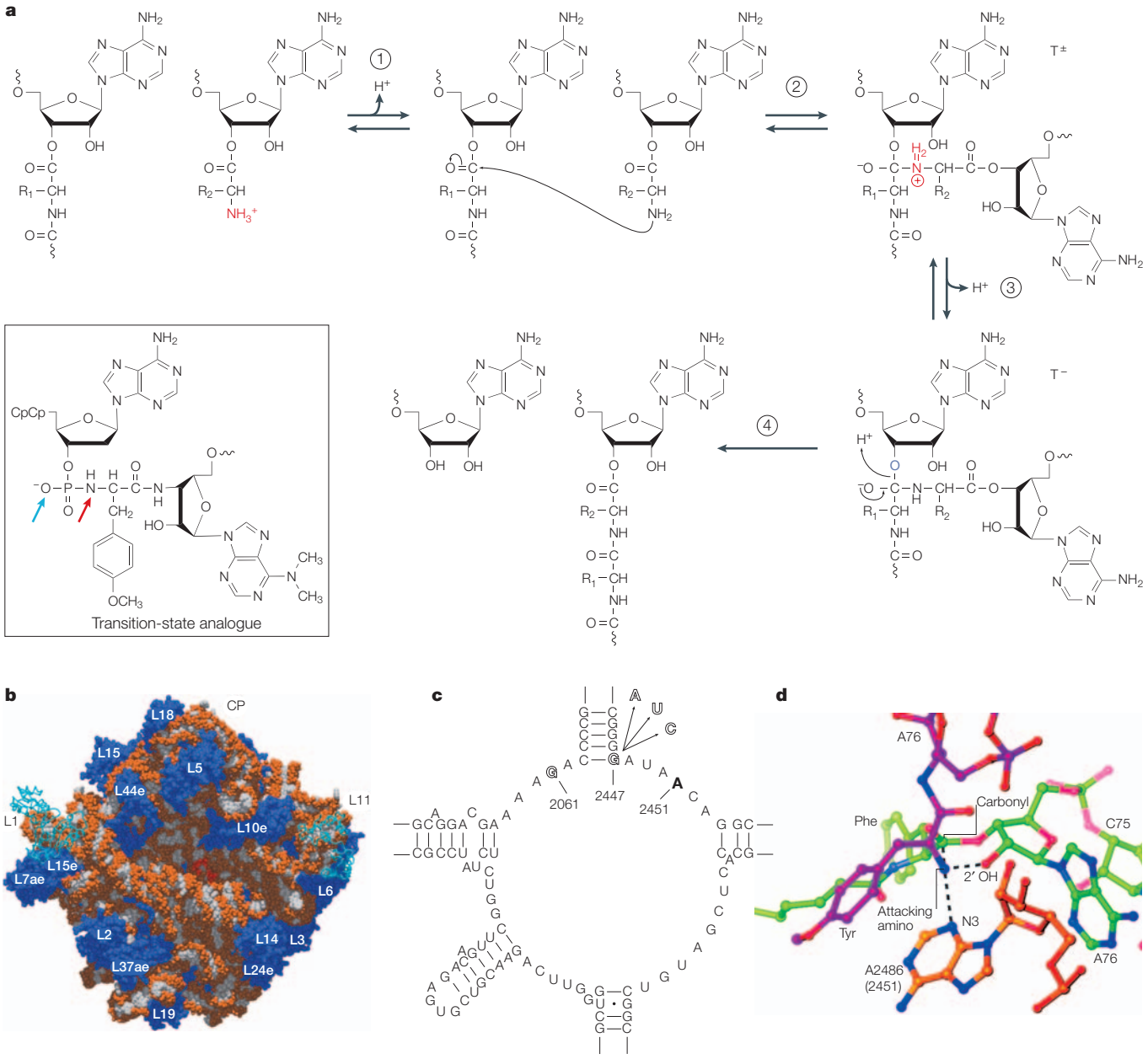

Figure 5 | **The ribosomal catalysis of protein synthesis. a** | Chemical mechanism of peptide-bond formation[22]. In the first step, the nucleophilic amine (NH_3^+; red) of the A-site aminoacyl-tRNA is activated by the loss of a proton. Next, the free amine attacks the carbonyl carbon of the aminoacyl ester of the P-site tRNA to produce a ZWITTERIONIC tetrahedral intermediate designated $T^{\pm}$, which then loses a proton to form a different intermediate, T^-. In the last step, protonation of the 3′-oxygen leaving group accompanies the breakdown of T^- to form products. Groups that lose a proton are shown in red and the group that gains a proton is shown in blue. The blue and red arrows indicate positions that correspond to the carbonyl oxygen and the nucleophilic amine, respectively, on the transition-state analogue that was used to locate the active site (boxed). CpCp represents further nucleotides that mimic the 3′ end of the tRNA. **b** | Structure of the 50S subunit from *Haloarcula marismortuii*[3]. The 23S rRNA is shown in red and white spacefill, whereas the ribosomal proteins are shown in dark blue spacefill. The lighter blue ribbon structures represent proteins that have been modelled from the electron-microscopy density and are not observed in the crystal structure. The peptidyl-transferase centre is located in the deep cleft at the centre of the structure. a, archaeal; e, eukaryotic. **c** | The conserved secondary structure at the heart of the peptidyl-transferase centre. Position A2451, the nucleotide that forms hydrogen-bonding interactions with the transition-state analogue, is shown in bold, and its interacting partners, guanine residues G2061 and G2447, are outlined. Arrows indicate mutations that have only minimal effects on peptide-bond formation[82]. The black filled circle represents a non-Watson–Crick base pair. **d** | Details of the structure of the peptidyl-transferase centre in complex with a puromycin-based transition-state analogue, which is shown in green (the other colours are used for contrast only)[104,105]. The N3 of A2451 (position A2451 of *Escherichia coli* rRNA is equivalent to A2486 of *H. marismortuii* rRNA) is in direct contact with the nascent peptide bond. Part **a** is modified with permission from REF. 22 © (2002) Elsevier. Part **b** is reproduced with permission from REF. 3 © (2000) The American Association for the Advancement of Science. Part **c** is reproduced with permission from *Nature* REF. 82 © (2001) Macmillan Magazines Ltd. Part **d** is reproduced with permission from REF. 105 © (2002) National Academy of Sciences, USA.

ZWITTERION
A dipolar ion that contains ionic groups of opposite charge, and has a net charge of zero.

been underappreciated. RNAs assemble in association with stoichiometric amounts of cations that are needed to neutralize phosphate charge, so the participation of ions in ribozyme activity will probably reflect more complex and subtle influences on the active-site architecture and catalytic chemistry than has been the case for protein metalloenzymes that bind to only one or a few metal cofactors.

To the delight of RNA enzymologists, who feared that the story of RNA catalysis would begin and end with divalent metals, RNA enzymes are turning out to use the same repertoire of catalytic strategies as protein enzymes — that is, general acid–base catalysis, electrostatic stabilization of the transition state, and destabilization of the ground state. The most striking advance in recent years has been the accumulation of high-resolution active-site structures that illustrate the degree to which RNA enzymes precisely orient and align reactive groups. The challenge for RNA biochemists will be to convert these snapshots into a comprehensive understanding of reaction pathways.

1. *The RNA World*, 2nd edn (eds Gesteland, R. F., Cech, T. R. & Atkins, J. F.) (Cold Spring Harbor Laboratory Press, New York, 1999).
2. Yusupov, M. M. *et al.* Crystal structure of the ribosome at 5.5 Å resolution. *Science* **292**, 883–896 (2001).
3. Nissen, P., Hansen, J., Ban, N., Moore, P. & Steitz, T. The structural basis of ribosome activity in peptide bond synthesis. *Science* **289**, 920–930 (2000).
The crystal structures of the large ribosomal subunit and of complexes with two substrate analogues demonstrate that the ribosome is a catalytic RNA and identify the nucleotide functional groups in the RNA active site.
4. Winkler, W. C., Nahvi, A., Roth, A., Collins, J. A. & Breaker, R. R. Control of gene expression by a natural metabolite-responsive ribozyme. *Nature* **428**, 281–286 (2004).
5. Teixeira, A. *et al.* Autocatalytic RNA cleavage in the human β-globin pre-mRNA promotes transcription termination. *Nature* **432**, 526–530 (2004).
6. Pley, H. W., Flaherty, K. M. & McKay, D. B. Three-dimensional structure of a hammerhead ribozyme. *Nature* **372**, 68–74 (1994).
7. Scott, W. G., Finch, J. T. & Klug, A. The crystal structure of an all-RNA hammerhead ribozyme: a proposed mechanism for RNA catalytic cleavage. *Cell* **81**, 991–1002 (1995).
8. Scott, W. G., Murray, J. B., Arnold, J. R., Stoddard, B. L. & Klug, A. Capturing the structure of a catalytic RNA intermediate: the hammerhead ribozyme. *Science* **274**, 2065–2069 (1996).
9. Murray, J. B., Szoke, H., Szoke, A. & Scott, W. G. Capture and visualization of a catalytic RNA enzyme–product complex using crystal lattice trapping and X-ray holographic reconstruction. *Mol. Cell* **5**, 279–287 (2000).
10. Scott, W. G. Visualizing the structure and mechanism of a small nucleolytic ribozyme. *Methods* **28**, 302–306 (2002).
11. Murray, J. B. *et al.* The structural basis of hammerhead ribozyme self-cleavage. *Cell* **92**, 665–673 (1998).
12. Scott, W. G. Biophysical and biochemical investigations of RNA catalysis in the hammerhead ribozyme. *Q. Rev. Biophys.* **32**, 241–284 (1999).
13. Ferré-D'Amaré, A. R., Zhou, K. & Doudna, J. A. Crystal structure of a hepatitis delta virus ribozyme. *Nature* **395**, 567–574 (1998).
The crystal structure of the 3′ product of the HDV ribozyme self-cleavage places C75 in a solvent-inaccessible cleft near the 5′-oxygen leaving group, where it might mediate general acid catalysis. There is no evidence of an active-site metal ion.
14. Ke, A., Zhou, K., Ding, F., Cate, J. H. & Doudna, J. A. A conformational switch controls hepatitis delta virus ribozyme catalysis. *Nature* **429**, 201–205 (2004).
The crystal structure of an uncleaved HDV ribozyme inactivated by a C75U mutation shows U75 near the 2′-oxygen nucleophile, where the wild-type C75 nucleotide base might mediate general base catalysis, and a divalent metal in position for a water-mediated interaction with the 5′-oxygen leaving group.
15. Rupert, P. B. & Ferré-D'Amaré, A. R. Crystal structure of a hairpin ribozyme–inhibitor complex with implications for catalysis. *Nature* **410**, 780–786 (2001).
The crystal structure of the hairpin ribozyme in complex with an uncleavable substrate analogue shows nucleophilic and leaving group oxygens in the appropriate alignment for an S_N2-type attack mechanism and places the Watson–Crick face of G8 near the reactive phosphate.
16. Rupert, P. B., Massey, A. P., Sigurdsson, S. T. & Ferré-D'Amaré, A. R. Transition state stabilization by a catalytic RNA. *Science* **298**, 1421–1424 (2002).
The crystal structure of a hairpin ribozyme complex with vanadate, a transition state mimic, shows interactions with functional groups on the Watson–Crick faces of G8 and A38.
17. Adams, P. L., Stahley, M. R., Kosek, A. B., Wang, J. & Strobel, S. A. Crystal structure of a self-splicing group I intron with both exons. *Nature* **430**, 45–50 (2004).
The crystal structure of a pre-tRNA intron with both exons that is inactivated by deoxynucleotide substitutions shows the 3′ oxygen of the 5′ exon in position for a nucleophilic attack on the reactive phosphate. The active site contains two of the three active-site metals that have been implicated in the catalysis of self-splicing by biochemical experiments.
18. Guo, F., Gooding, A. R. & Cech, T. R. Structure of the *Tetrahymena* ribozyme: base triple sandwich and metal ion at the active site. *Mol. Cell* **16**, 351–362 (2004).
19. Adams, P. L. *et al.* Crystal structure of a group I intron splicing intermediate. *RNA* **10**, 1867–1887 (2004).
20. Golden, B. L., Kim, H. & Chase, E. Crystal structure of a phage Twort group I ribozyme–product complex. *Nature Struct. Mol. Biol.* **12**, 82–89 (2005).
21. Moore, P. B. & Steitz, T. A. After the ribosome structures: how does peptidyl transferase work? *RNA* **9**, 155–159 (2003).
22. Green, R. & Lorsch, J. R. The path to perdition is paved with protons. *Cell* **110**, 665–668 (2002).
23. Benkovic, S. & Schray, K. in *The Enzymes* Vol. 8 (ed. Boyer, P. D.) 201–238 (Academic Press, New York, 1973).
24. Knowles, J. R. Enzyme-catalyzed phosphoryl transfer reactions. *Annu. Rev. Biochem.* **49**, 877–919 (1980).
25. Steitz, T. A. & Steitz, J. A. A general two-metal mechanism for catalytic RNA. *Proc. Natl Acad. Sci. USA* **90**, 6498–6502 (1993).
26. Shih, I. & Been, M. D. Catalytic strategies of the hepatitis delta virus ribozymes. *Annu. Rev. Biochem.* **71**, 887–917 (2002).
27. Ferré-D'Amaré, A. R. & Doudna, J. A. Crystallization and structure determination of a hepatitis delta virus ribozyme: use of the RNA-binding protein U1A as a crystallization module. *J. Mol. Biol.* **295**, 541–556 (2000).
28. Hampel, A. & Cowan, J. A. A unique mechanism for RNA catalysis: the role of metal cofactors in hairpin ribozyme cleavage. *Chem. Biol.* **4**, 513–517 (1997).
29. Nesbitt, S., Hegg, L. A. & Fedor, M. J. An unusual pH-independent and metal-ion-independent mechanism for hairpin ribozyme catalysis. *Chem. Biol.* **4**, 619–630 (1997).
30. Young, K. J., Gill, F. & Grasby, J. A. Metal ions play a passive role in the hairpin ribozyme catalysed reaction. *Nucleic Acids Res.* **25**, 3760–3766 (1997).
31. Murray, J. B., Seyhan, A. A., Walter, N. G., Burke, J. M. & Scott, W. G. The hammerhead, hairpin and VS ribozymes are catalytically proficient in monovalent cations alone. *Chem. Biol.* **5**, 587–595 (1998).
32. Perrotta, A. T., Shih, I. & Been, M. D. Imidazole rescue of a cytosine mutation in a self-cleaving ribozyme. *Science* **286**, 123–126 (1999).
33. Lupták, A., Ferré-D'Amaré, A. R., Zhou, K., Zilm, K. W. & Doudna, J. A. Direct pK_a measurement of the active-site cytosine in a genomic hepatitis delta virus ribozyme. *J. Am. Chem. Soc.* **123**, 8447–8452 (2001).
34. Oyelere, A. K., Kardon, J. R. & Strobel, S. A. pK_a perturbation in genomic hepatitis delta virus ribozyme catalysis evidenced by nucleotide analogue interference mapping. *Biochemistry* **41**, 3667–3675 (2002).
35. Nakano, S., Chadalavada, D. M. & Bevilacqua, P. C. General acid–base catalysis in the mechanism of a hepatitis delta virus ribozyme. *Science* **287**, 1493–1497 (2000).
36. Shih, I. & Been, M. D. Involvement of a cytosine side chain in proton transfer in the rate-determining step of ribozyme self-cleavage. *Proc. Natl Acad. Sci. USA* **98**, 1489–1494 (2001).
Changes in the pH-rate profiles that result from cytosine mutations and the rescue of cytosine mutations with exogenous imidazole analogues implicate an active-site cytosine in general acid–base catalysis of HDV ribozyme self-cleavage.
37. Toney, M. & Kirsch, J. Direct Brønsted analysis of the restoration of activity to a mutant enzyme by exogenous amines. *Science* **243**, 1485–1488 (1989).
38. Jencks, W. P. *Catalysis in Chemistry and Enzymology* 163–242 (Dover Publications, New York, 1969).
39. Nakano, S., Proctor, D. J. & Bevilacqua, P. C. Mechanistic characterization of the HDV genomic ribozyme: assessing the catalytic and structural contributions of divalent metal ions within a multichannel reaction mechanism. *Biochemistry* **40**, 12022–12038 (2001).
40. Fedor, M. J. Structure and function of the hairpin ribozyme. *J. Mol. Biol.* **297**, 269–291 (2000).
41. Walter, N. G., Hampel, K. J., Brown, K. M. & Burke, J. M. Tertiary structure formation in the hairpin ribozyme monitored by fluorescence resonance energy transfer. *EMBO J.* **17**, 2378–2391 (1998).
42. Walter, N. G., Burke, J. M. & Millar, D. P. Stability of hairpin ribozyme tertiary structure is governed by the interdomain junction. *Nature Struct. Biol.* **6**, 544–549 (1999).
43. Zhao, Z., Wilson, T., Maxwell, K. & Lilley, D. The folding of the hairpin ribozyme: dependence on the loops and the junction. *RNA* **6**, 1833–1846 (2000).
44. Hampel, A. & Tritz, R. RNA catalytic properties of the minimum (–)sTRSV sequence. *Biochemistry* **28**, 4929–4933 (1989).
45. Fedor, M. J. Tertiary structure stabilization promotes hairpin ribozyme ligation. *Biochemistry* **38**, 11040–11050 (1999).
46. Yadava, R., Choi, A., Lebruska, L. & Fedor, M. Hairpin ribozymes with four-way helical junctions mediate intracellular RNA ligation. *J. Mol. Biol.* **309**, 893–902 (2001).
47. Klostermeier, D. & Millar, D. P. Tertiary structure stability of the hairpin ribozyme in its natural and minimal forms: different energetic contributions from a ribose zipper motif. *Biochemistry* **40**, 11211–11218 (2001).
48. Ferré-D'Amaré, A. R. & Rupert, P. B. The hairpin ribozyme: from crystal structure to function. *Biochem. Soc. Trans.* **30**, 1105–1109 (2001).
49. Ryder, S. P. & Strobel, S. A. Comparative analysis of hairpin ribozyme structures and interference data. *Nucleic Acids Res.* **30**, 1287–1291 (2002).
50. Ferré-D'Amaré, A. R. The hairpin ribozyme. *Biopolymers* **73**, 71–78 (2004).
51. van Tol, H., Buzayan, J. M., Feldstein, P. A., Eckstein, F. & Bruening, G. Two autolytic processing reactions of a satellite RNA proceed with inversion of configuration. *Nucleic Acids Res.* **18**, 1971–1975 (1990).
52. Bevilacqua, P. C. Mechanistic considerations for general acid–base catalysis by RNA: revisiting the mechanism of the hairpin ribozyme. *Biochemistry* **42**, 2259–2265 (2003).
53. Pinard, R. *et al.* Functional involvement of G8 in the hairpin ribozyme cleavage mechanism. *EMBO J.* **20**, 6434–6442 (2001).
54. Kuzmin, Y. I., Da Costa, C. C. & Fedor, M. J. Role of an active site guanine in hairpin ribozyme catalysis probed by exogenous nucleobase rescue. *J. Mol. Biol.* **340**, 233–251 (2004).
55. Lebruska, L. L., Kuzmine, I. I. & Fedor, M. J. Rescue of an abasic hairpin ribozyme by cationic nucleobases. Evidence for a novel mechanism of RNA catalysis. *Chem. Biol.* **9**, 465–473 (2002).
56. Kuzmin, Y. I., DaCosta, C. P., Cottrell, J. & Fedor, M. J. Contribution of an active site adenosine to hairpin ribozyme catalysis. *J. Mol. Biol.* (in the press).

57. Hutchins, C. J., Rathjen, P. D., Forster, A. C. & Symons, R. H. Self-cleavage of plus and minus transcripts of avocado sunblotch viroid. *Nucleic Acids Res.* **14**, 3627–3640 (1986).
58. Buzayan, J. M., Gerlach, W. L. & Bruening, G. Nonenzymatic cleavage and ligation of RNAs complementary to a plant virus satellite RNA. *Nature* **323**, 349–353 (1986).
59. Burke, J. M. Hairpin and hammerhead ribozymes: how different are they? *Biochem. Soc. Trans.* **30**, 1115–1118 (2002).
60. Blount, K. F. & Uhlenbeck, O. C. The hammerhead ribozyme. *Biochem. Soc. Trans.* **30**, 1119–1122 (2002).
61. Hammann, C. & Lilley, D. M. Folding and activity of the hammerhead ribozyme. *Chembiochem* **3**, 690–700 (2002).
62. Blount, K. F. & Uhlenbeck, O. C. The structure–function dilemma for the hammerhead ribozyme. *Annu. Rev. Biophys. Biomol. Struct.* (in the press).
63. McKay, D. B. Structure and function of the hammerhead ribozyme: an unfinished story. *RNA* **2**, 395–403 (1996).
64. Peracchi, A., Beigelman, L., Scott, E. C., Uhlenbeck, O. C. & Herschlag, D. Involvement of a specific metal ion in the transition of the hammerhead ribozyme to its catalytic conformation. *J. Biol. Chem.* **272**, 26822–26826 (1997).
65. Wang, S., Karbstein, K., Peracchi, A., Beigelman, L. & Herschlag, D. Identification of the hammerhead ribozyme metal ion binding site responsible for rescue of the deleterious effect of a cleavage site phosphorothioate. *Biochemistry* **38**, 14363–14378 (1999).
66. Khvorova, A., Lescoute, A., Westhof, E. & Jayasena, S. D. Sequence elements outside the hammerhead ribozyme catalytic core enable intracellular activity. *Nature Struct. Biol.* **10**, 708–712 (2003).
67. De la Pena, M., Gago, S. & Flores, R. Peripheral regions of natural hammerhead ribozymes greatly increase their self-cleavage activity. *EMBO J.* **22**, 5561–5570 (2003).
68. Penedo, J. C., Wilson, T. J., Jayasena, S. D., Khvorova, A. & Lilley, D. M. Folding of the natural hammerhead ribozyme is enhanced by interaction of auxiliary elements. *RNA* **10**, 880–888 (2004).
69. Canny, M. D. *et al.* Fast cleavage kinetics of a natural hammerhead ribozyme. *J. Am. Chem. Soc.* **126**, 10848–10849 (2004).
70. Saksmerprome, V., Roychowdhury-Saha, M., Jayasena, S., Khvorova, A. & Burke, D. H. Artificial tertiary motifs stabilize *trans*-cleaving hammerhead ribozymes under conditions of submillimolar divalent ions and high temperatures. *RNA* **10**, 1916–1924 (2004).
71. Cech, T. R. & Golden, B. L. in *The RNA World*, 2nd edn (eds Gesteland, R. F., Cech, T. R. & Atkins, J. F.) 321–349 (Cold Spring Harbor Laboratory Press, New York, 1999).
72. Horton, N. C. & Perona, J. J. Making the most of metal ions. *Nature Struct. Biol.* **8**, 290–293 (2001).
73. Fedor, M. J. The role of metal ions in RNA catalysis. *Curr. Opin. Struct. Biol.* **12**, 289–295 (2002).
74. Weinstein, L. B., Jones, B. C., Cosstick, R. & Cech, T. R. A second catalytic metal ion in group I ribozyme. *Nature* **388**, 805–808 (1997).
75. Shan, S. & Herschlag, D. Probing the role of metal ions in RNA catalysis: kinetic and thermodynamic characterization of a metal ion interaction with the 2′-moiety of the guanosine nucleophile in the *Tetrahymena* group I ribozyme. *Biochemistry* **38**, 10958–10975 (1999).
76. Shan, S., Yoshida, A., Sun, S., Piccirilli, J. A. & Herschlag, D. Three metal ions at the active site of the *Tetrahymena* group I ribozyme. *Proc. Natl Acad. Sci. USA* **96**, 12299–12304 (1999).
Metal-cation specificity-switch experiments support a three-metal mechanism of group-I intron splicing, in which three distinct metal cations interact with the 3′ oxygen of the oligonucleotide substrate and the 3′ and 2′ oxygens of the guanosine nucleophile.
77. Yoshida, A., Sun, S. & Piccirilli, J. A. A new metal ion interaction in the *Tetrahymena* ribozyme reaction revealed by double sulfur substitution. *Nature Struct. Biol.* **6**, 318–321 (1999).
78. Shan, S., Kravchuk, A. V., Piccirilli, J. A. & Herschlag, D. Defining the catalytic metal ion interactions in the *Tetrahymena* ribozyme reaction. *Biochemistry* **40**, 5161–5171 (2001).
79. Sjögren, A. S., Pettersson, E., Sjöberg, B. M. & Strömberg, R. Metal ion interaction with cosubstrate in self-splicing of group I introns. *Nucleic Acids Res.* **25**, 648–653 (1997).
80. Noller, H. F., Hoffarth, V. & Zimniak, L. Unusual resistance of peptidyl transferase to protein extraction methods. *Science* **256**, 1416–1419 (1992).
81. Muth, G., Ortoleva-Donnelly, L. & Strobel, S. A single adenosine with a neutral pK_a in the ribosomal peptidyl transferase center. *Science* **289**, 947–950 (2000).
82. Polacek, N., Gaynor, M., Yassin, A. & Mankin, A. S. Ribosomal peptidyl transferase can withstand mutations at the putative catalytic nucleotide. *Nature* **411**, 498–501 (2001).
83. Muth, G. W., Chen, L., Kosek, A. B. & Strobel, S. A. pH-dependent conformational flexibility within the ribosomal peptidyl transferase center. *RNA* **7**, 1403–1415 (2001).
84. Katunin, V. I., Muth, G. W., Strobel, S. A., Wintermeyer, W. & Rodnina, M. V. Important contribution to catalysis of peptide bond formation by a single ionizing group within the ribosome. *Mol. Cell* **10**, 339–346 (2002).
85. Rodnina, M. V. & Wintermeyer, W. Peptide bond formation on the ribosome: structure and mechanism. *Curr. Opin. Struct. Biol.* **13**, 334–340 (2003).
86. Sievers, A., Beringer, M., Rodnina, M. V. & Wolfenden, R. The ribosome as an entropy trap. *Proc. Natl Acad. Sci. USA* **101**, 7897–7901 (2004).
87. Weinger, J. S., Parnell, K. M., Dorner, S., Green, R. & Strobel, S. A. Substrate-assisted catalysis of peptide bond formation by the ribosome. *Nature Struct. Mol. Biol.* **11**, 1101–1106 (2004).
88. Youngman, E. M., Brunelle, J. L., Kochaniak, A. B. & Green, R. The active site of the ribosome is composed of two layers of conserved nucleotides with distinct roles in peptide bond formation and peptide release. *Cell* **117**, 589–599 (2004).
89. Perrault, D. M. & Anslyn, E. V. Unifying the current data on the mechanism of cleavage-transesterification of RNA. *Angew. Chem. Int. Ed. Engl.* **36**, 432–450 (1997).
90. Raines, R. T. Ribonuclease A. *Chem. Rev.* **98**, 1045–1066 (1998).
91. Oivanen, M., Kuusela, S. & Lönnberg, H. Kinetics and mechanisms for the cleavage and isomerization of the phosphodiester bonds of RNA by Brønsted acids and bases. *Chem. Rev.* **98**, 961–990 (1998).
92. Lister, J. H. in *Fused pyrimidines* Vol. 24 (ed. Brown, D. J.) 478–496 (John Wiley & Sons, New York, 1971).
93. Brown, D. J. in *The Pyrimidines* Vol. 52 (ed. Taylor, E. G.) 823–853 (John Wiley & Sons, New York, 1994).
94. Kochetkov, N. K. & Budovskii, E. I. in *Organic Chemistry of Nucleic Acids* (eds Kochetkov, N. K. & Budovskii, E. I.) 148–165 (Plenum, New York, 1971).
95. Narlikar, G. J. & Herschlag, D. Mechanistic aspects of enzymatic catalysis: lessons from comparison of RNA and protein enzymes. *Annu. Rev. Biochem.* **66**, 19–59 (1997).
96. Bevilacqua, P. C., Brown, T. S., Nakano, S. & Yajima, R. Catalytic roles for proton transfer and protonation in ribozymes. *Biopolymers* **73**, 90–109 (2004).
97. Draper, D. E. A guide to ions and RNA structure. *RNA* **10**, 335–343 (2004).
98. Draper, D. E., Grilley, D. & Soto, A. M. Ions and RNA folding. *Annu. Rev. Biophys. Biomol. Struct.* 29 Oct 2004 [epub ahead of print].
99. Sigel, R. K. O., Song, B. & Sigel, H. Stabilities and structures of metal ion complexes of adenosine 5′-*O*-thiomonophosphate ($AMPS^{2-}$) in comparison with those of its parent nucleotide (AMP^{2-}) in aqueous solution. *J. Am. Chem. Soc.* **119**, 744–755 (1997).
100. Frey, P. A. & Sammons, R. D. Bond order and charge localization in nucleoside phosphorothioates. *Science* **228**, 541–545 (1985).
101. Basu, S. & Strobel, S. A. Thiophilic metal ion rescue of phosphorothioate interference within the *Tetrahymena* ribozyme P4–P6 domain. *RNA* **5**, 1399–1407 (1999).
102. Doherty, E. A. & Doudna, J. A. Ribozyme structures and mechanisms. *Annu. Rev. Biochem.* **69**, 597–615 (2000).
103. Golden, B. L., Gooding, A. R., Podell, E. R. & Cech, T. R. A preorganized active site in the crystal structure of the *Tetrahymena* ribozyme. *Science* **282**, 259–264 (1998).
104. Steitz, T. A. & Moore, P. B. RNA, the first macromolecular catalyst: the ribosome is a ribozyme. *Trends Biochem. Sci.* **28**, 411–418 (2003).
105. Hansen, J. L., Schmeing, T. M., Moore, P. B. & Steitz, T. A. Structural insights into peptide bond formation. *Proc. Natl Acad. Sci. USA* **99**, 11670–11675 (2002).

Acknowledgements

Work in our laboratories is supported by grants from the National Institutes of Health and by the Skaggs Institute for Chemical Biology.

Competing interests statement

The authors declare no competing financial interests.

Online links

FURTHER INFORMATION

James Williamson's laboratory: http://www.scripps.edu/research/faculty.php?tsri_id=5676

Martha Fedor's laboratory: http://www.scripps.edu/research/faculty.php?tsri_id=5677

RNABase.org: The RNA Structure Database: http://www.rnabase.org

Access to this interactive links box is free online.